Received: 21 February 2021 | Revised: 28 July 2021 | Accepted: 16 August 2021

DOI: 10.1002/mrm.28998

RESEARCH ARTICLE

Magnetic Resonance in Medicine

Quantitative evaluation of prospective motion correction in healthy subjects at 7T MRI

Alessandro Sciarra[1,2,3] | **Hendrik Mattern**[2] | **Renat Yakupov**[4] | **Soumick Chatterjee**[2,5] | **Daniel Stucht**[2] | **Steffen Oeltze-Jafra**[1,4,6] | **Frank Godenschweger**[2] | **Oliver Speck**[2,3,4,6,7]

[1]Medicine and Digitalization–MedDigit, Medical Faculty, University Department of Neurology, Otto von Guericke University, Magdeburg, Germany

[2]Department of Biomedical Magnetic Resonance, Otto von Guericke University, Magdeburg, Germany

[3]Institute for Physics, Otto von Guericke University, Magdeburg, Germany

[4]German Centre for Neurodegenerative Diseases, Magdeburg, Germany

[5]Data and Knowledge Engineering Group, Faculty of Computer Science, Otto von Guericke University, Magdeburg, Germany

[6]Center for Behavioral Brain Sciences, Magdeburg, Germany

[7]Leibniz Institute for Neurobiology, Magdeburg, Germany

Correspondence
Alessandro Sciarra, Medicine and Digitalization–MedDigit, Medical Faculty, University Department of Neurology, Otto von Guericke University, Leipziger Str. 44, 39120 Magdeburg, Germany.
Email: alessandro.sciarra@med.ovgu.de

Funding information
Initial Training Network, funded by the FP7 Marie Curie Actions of the European Commission (FP7-PEOPLE-2012-ITN-316716) and the National Institutes of Health (1R01-DA021146), the DFG (DFG-MA 9235/1-1), and the federal state of Saxony-Anhalt ("I 88")

Purpose: Quantitative assessment of prospective motion correction (PMC) capability at 7T MRI for compliant healthy subjects to improve high-resolution images in the absence of intentional motion.

Methods: Twenty-one healthy subjects were imaged at 7 T. They were asked not to move, to consider only unintentional motion. An in-bore optical tracking system was used to monitor head motion and consequently update the imaging volume. For all subjects, high-resolution T_1 (3D-MPRAGE), T_2 (2D turbo spin echo), proton density (2D turbo spin echo), and T_2^* (2D gradient echo) weighted images were acquired with and without PMC. The images were evaluated through subjective and objective analysis.

Results: Subjective evaluation overall has shown a statistically significant improvement (5.5%) in terms of image quality with PMC ON. In a separate evaluation of every contrast, three of the four contrasts (T_1, T_2, and proton density) have shown a statistically significant improvement (9.62%, 9.85%, and 9.26%), whereas the fourth one (T_2^*) has shown improvement, although not statistically significant. In the evaluation with objective metrics, average edge strength has shown an overall improvement of 6% with PMC ON, which was statistically significant; and gradient entropy has shown an overall improvement of 2%, which did not reach statistical significance.

Conclusion: Based on subjective assessment, PMC improved image quality in high-resolution images of healthy compliant subjects in the absence of intentional motion for all contrasts except T_2^*, in which no significant differences were observed. Quantitative metrics showed an overall trend for an improvement with PMC, but not all differences were significant.

KEYWORDS
high-resolution structural MRI, image quality assessment, optical motion tracking system, PMC, ultrahigh field

1 | INTRODUCTION

With the growing use of ultrahigh-field MRI, higher spatial resolutions can be achieved. With increasing resolution, more phase-encoding steps are required, while at the same time the available SNR decreases. Thus, high-resolution imaging (isotropic voxel size ≤ 0.5 mm^3) can require longer scan time (several tens of minutes). During these lengthy high-resolution acquisitions, even compliant subjects move unintentionally (ie, due to breathing and muscle relaxation).[1,2] For high-resolution imaging, the amplitude of these unintentional motions is on the scale of the voxel size (hence, can introduce image artifacts, which effectively negate the advantage of high resolution). With prospective motion correction (PMC),[3] it is possible to limit the image degradation caused by head motion.[1,4,5] The PMC uses position and orientation tracking data of the head in 3D space to update the imaging volume in real time.[6] The tracking data can be obtained in various ways, differing in terms of accuracy and precision.[4,7-11] For high-resolution MRI, PMC with Moiré phase tracking (MPT)—an external, in-bore, optical tracking system—is currently considered the gold standard[12,13] and was therefore used in this study. This MPT system was used in several high-resolution studies and showed image improvements, both qualitatively and quantitatively, when motion is corrected prospectively.[1,14-16] However, these studies focused on a single contrast and included only small cohorts (1-11 subjects). Thus, a comprehensive assessment of the performance of PMC for high-resolution MRI in a larger cohort is missing. To that end, we acquired data of 21 healthy subjects for four different sequences at 7 T. To mimic a routine research setting, subjects were asked not to move (unlike most motion-correction studies that correct for intentional motion). The images were assessed subjectively through expert ratings and objectively with image metrics. The aim of this work was to verify and quantify whether PMC can significantly improve image quality at 7 T, for healthy compliant subjects and in the regime of "quasi-no-motion" as introduced by Stucht et al.[1] This study is not meant to assess the performance of PMC for a broader population of subjects inexperienced with MRI.

2 | METHODS

Twenty-one healthy subjects (14 males, 31.5 ± 6.1 years, and 7 females, 27.3 ± 3.4 years), were scanned in two separate sessions, each with a duration of 75 minutes. The procedures were approved by the local ethics committee, and all subjects provided informed written consent before participation. Scanning was performed with a 7T whole-body MRI scanner (Siemens Healthineers, Erlangen, Germany) using a 32-channel head coil (Nova Medical, Wilmington, MA) and an optical motion tracking system (OMTS) that consisted of an MR compatible camera (MT384i, Metria Innovation Inc., Milwaukee, WI, USA) and a Moiré Phase Tracking (MPT) marker (Metria Innovation Inc., Milwaukee, WI, USA), Figure 1.

2.1 | Optical motion tracking system and MR sequences

The operational principle of the Optical Motion Tracking System (OMTS) is the detection of the 3D position (x, y, and z) and orientation (Pitch, Yaw, Roll) based on the Moiré phase patterns generated by the MPT marker (Figure 1). A dental impression was tailor-made for each subject to produce a personalized mouthpiece to which the MPT marker was attached (Figure 1).[1] The use of personal mouthpieces facilitates a rigid coupling, and thus prevents pseudo motion. All participants were previously imaged at 3T MRI, and at least 66% of the participants were also imaged at 7 T. Four subjects also had a precedent experience with PMC. None of the subjects ever reported any kind of problem with the mouthpiece, nor has there been any kind of complaint during or after the scan sessions. The in-bore camera was mounted and unmounted for each session using Velcro straps (Figure 1). The optical camera was set to acquire 80 frames/second, and the marker was tracked with a precision of 0.01 mm and 0.01°, for translations (x, y, z) and rotations (α, β, and γ, corresponding to Pitch, Yaw, and Roll), respectively.[17] Tracking data, position, and orientation, once extracted from each frame (with a separate control computer), were continuously sent to the MRI scanner to update the imaging volume once per TR, before each excitation.

Before use in human subjects, the tracking system was calibrated following the procedure proposed by Zaitsev et al.[8]

All of the sequences were tested on a phantom to check the image quality for a nonmoving object. In addition, we evaluated the impact of mechanical vibrations produced by gradients during scans on the OMTS. This was done by scanning a stationary phantom with the same sequences used in vivo and motion correction enabled.

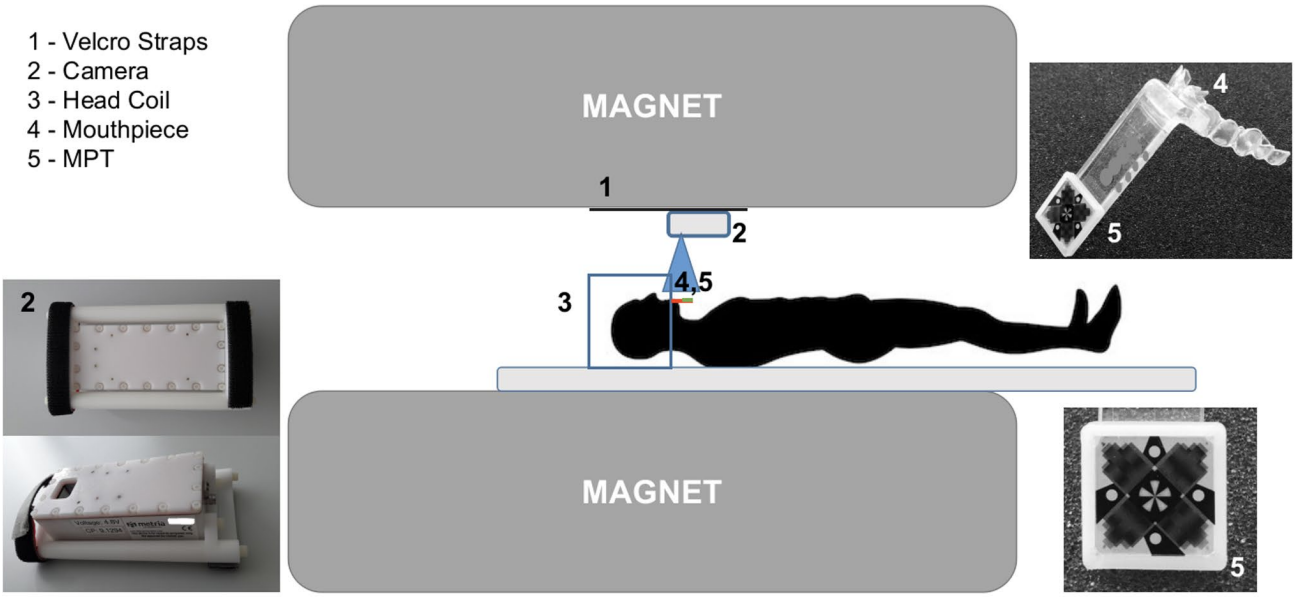

FIGURE 1 Optical motion tracking system (OMTS). The camera (2) has two Velcro straps. Additional Velcro straps (1) are permanently glued to the bore of the scanner, enabling the mounting and unmounting of the camera when necessary. The blue square represents the head coil (3), and the red line represents the mouthpiece (4) and the Moiré Phase Tracking (MPT) marker (5)

TABLE 1 Sequence parameters

Sequence	3D-MPRAGE	2D-TSE	2D-TSE	2D-GRE	2D-GRE	2D-GRE
Contrast	T_1	T_2	PD	T_2^*	T_2^*	T_2^*
PMC	On/Off	On/Off	On/Off	On/Off	On/Off	On/Off
In-plane resolution (mm)	0.45 iso	0.28 iso	0.28 iso	0.5 iso	0.35 iso	0.25 iso
Slice thickness (mm)	0.45	1.0	1.0	1.5	1.5	1.5
Matrix size (voxel)	496 × 496	690 × 704	690 × 704	336 × 448	480 × 640	672 × 896
Voxel volume (mm^3)	0.091	0.078	0.078	0.375	0.184	0.094
slices	416	15	15	30	30	30
TR (ms)	2820	6000	6000	680	680	680
TE (ms)	2.82	59.0	9.9	16.6	15.1	16.6
TI (ms)	1050	—	—	—	—	—
Flip angle (°)	5	130	130	30	30	30
Bandwidth (Hz/px)	170	473	473	60	60	60
Total ADC duration (ms)	5.88	2.11	2.11	16.67	16.67	16.67
TA (mm:ss)	12:12	5:12	5:12	8:21	11:37	15:58
Parallel imaging	GRAPPA 2	GRAPPA 2	GRAPPA 2	GRAPPA 2	GRAPPA 2	GRAPPA 2

Abbreviations: GRE, gradient echo; iso, isotropic; TA, acquisition time; TSE, turbo spin echo.

The sequences used in this study were developed in previous studies that made use of PMC.[1] The contrasts acquired were proton density (PD), T_2, T_1, and T_2^*. The PD and T_2 were acquired using a 2D turbo spin-echo sequence, both with an in-plane resolution of 0.28 × 0.28 mm^2 and a slice thickness of 1.0 mm. The T_1-weighted images were acquired using a 3D-MPRAGE sequence with an isotropic resolution of 0.45 mm^3. The T_2^*-weighted images were acquired with a 2D gradient-echo (FLASH) sequence with three different in-plane resolutions: 0.25 × 0.25, 0.35 × 0.35 and 0.5 × 0.5 mm^2, keeping the slice thickness constant at 1.5 mm, referred henceforth as T_2^*−w (025), T_2^*−w (035), and T_2^*−w (05). All of the sequences and respective parameters used are summarized in Table 1. As mentioned previously, there

were two separate sessions on different dates: the first one for the acquisition of T_1, T_2, and PD scans; and the second for the remaining T_2^* scans. Within each session, the order of acquired sequences and application of PMC was randomized. The subjects were explicitly instructed to remain as stationary as possible during every scan. For the entire cohort, the total number of image volumes acquired was 252. The motion-tracking information, both with PMC OFF and ON, was stored in separate log files. For each contrast, separately for PMC OFF and ON, the tracking information was averaged to calculate the global mean and SD for every degree of freedom. Statistical analyses of displacements and rotations were calculated using the following equations:

$$\begin{aligned} &\Delta X = \left\{x_{i+\delta t} - x_i\right\}_{i=1,\ldots,n-1},\ \Delta Y = \left\{y_{i+\delta t} - y_i\right\}_{i=1,\ldots,n-1},\\ &\Delta Z = \left\{z_{i+\delta t} - z_i\right\}_{i=1,\ldots,n-1}\\ &\Delta A = \left\{\alpha_{i+\delta t} - \alpha_i\right\}_{i=1,\ldots,n-1},\ \Delta B = \left\{\beta_{i+\delta t} - \beta_i\right\}_{i=1,\ldots,n-1},\\ &\Delta \Gamma = \left\{\gamma_{i+\delta t} - \gamma_i\right\}_{i=1,\ldots,n-1} \end{aligned} \quad (1)$$

where ΔX, ΔY, ΔZ, ΔA, ΔB, and ΔΓ are arrays containing the displacements and rotations completed in the time $\delta t = 1$ second, and n is the number of time points of each sequence. The histograms for each of these arrays were calculated, and a statistical analysis was performed using the Mann–Whitney U test.[18]

To avoid possible bias in the assessment between PMC OFF versus ON, the scans (Off/On) that presented strongly different motion patterns in the same subject were excluded (ie, if the subject moved much more or much less during one of the acquisitions). Figure 2 portrays the workflow followed to exclude scans that showed different motion:

a. Motion patterns recorded by the OMTS;
b. Calculation of the distributions (see Equation 1), mean, and SD values for each degree of freedom;
c. Average of SDs for displacements and rotations;
d. Calculation of the motion parameter ratio between scans: $\frac{\sigma_{PMC-ON}}{\sigma_{PMC-OFF}}$, selection of subjects with similar motion patterns (ie, ratio of 1 ± 0.5), and exclusion of subjects where this ratio was smaller than 0.5 or larger than 1.5.

2.2 | Subjective image-quality assessment

Subjective assessments of image quality were performed by four neuroscientists, having at least 5 years of experience in working with MR image processing and image-quality assessment. The raters scored the image quality, looking in particular at the level of corruption due to motion artifacts. Scans were subdivided into six different groups, one for each contrast and for each in-plane resolution, as in the case of T_2^*-w images. A blinded side-by-side comparison (the order of presentation of two images with and without PMC was randomized) was done by each rater. The raters scored every scan by answering the following question: "Please rate the image quality considering the presence of motion artifacts from 1 to 10," where 1 corresponds to the worst image quality (highest presence of motion artifacts), and 10 to the best image quality (no motion artifacts). The only instruction given to the raters was to score the image quality in a paired (side-by-side) comparison, assigning the scores to both image volumes. To assess the agreement across raters, the intraclass correlation coefficient was calculated[19,20] using Pingouin[21] (Figure 3).

2.3 | Objective image-quality assessment

Several metrics for quantitative MR image-quality assessment or evaluation of the presence of motion artifacts have been proposed.[5,22-24] The MRIQC tool[22] is a valuable resource for automated quality assessment, but it primarily addresses T_1 and T_2 contrast image volumes acquired at lower magnetic fields (1.5 T and 3 T). The framework proposed by Pannetier et al for PMC evaluation makes use of two indicators: the average edge strength (AES) that quantifies the image blurring at edges and a Haralick texture-based indicator.[5] Gradient entropy is also commonly used to quantify differences in terms of quality for MR images.[23] In this study, AES and gradient entropy were used as metrics to judge the image quality quantitatively. The AES values decrease with increasing motion artifacts, and the gradient entropy values increase with an increasing level of corruption.[5,23] The Mann–Whitney U test was applied for the statistical analysis of the results.[18]

3 | RESULTS

For each of the quality assessments, there were three possible scenarios. First, the images acquired with PMC were visibly better than the images of the same subject obtained with the same sequence but acquired without PMC; second, images acquired with and without PMC had the same or nearly the same image quality; third, the images acquired with PMC were worse than those acquired without PMC support. In Figure 4, examples of the results obtained with and without PMC illustrate these three possible scenarios.

Following the scheme discussed earlier (see section 2.1; Figure 2), few subjects were excluded from each group. For example, T_1-w images of Sub-ID 16 were excluded because the subject moved too much during the acquisition with PMC ON, as shown in Figure 2. Similarly, Sub-IDs 4, 6, 13, and 18 for T_2-w; 4, 6, 15, and 18 for PD; 6 for T_2^*−w (05); 6, 15, and 16 for T_2^*−w (035); and finally, 20 for T_2^*−w (025) were

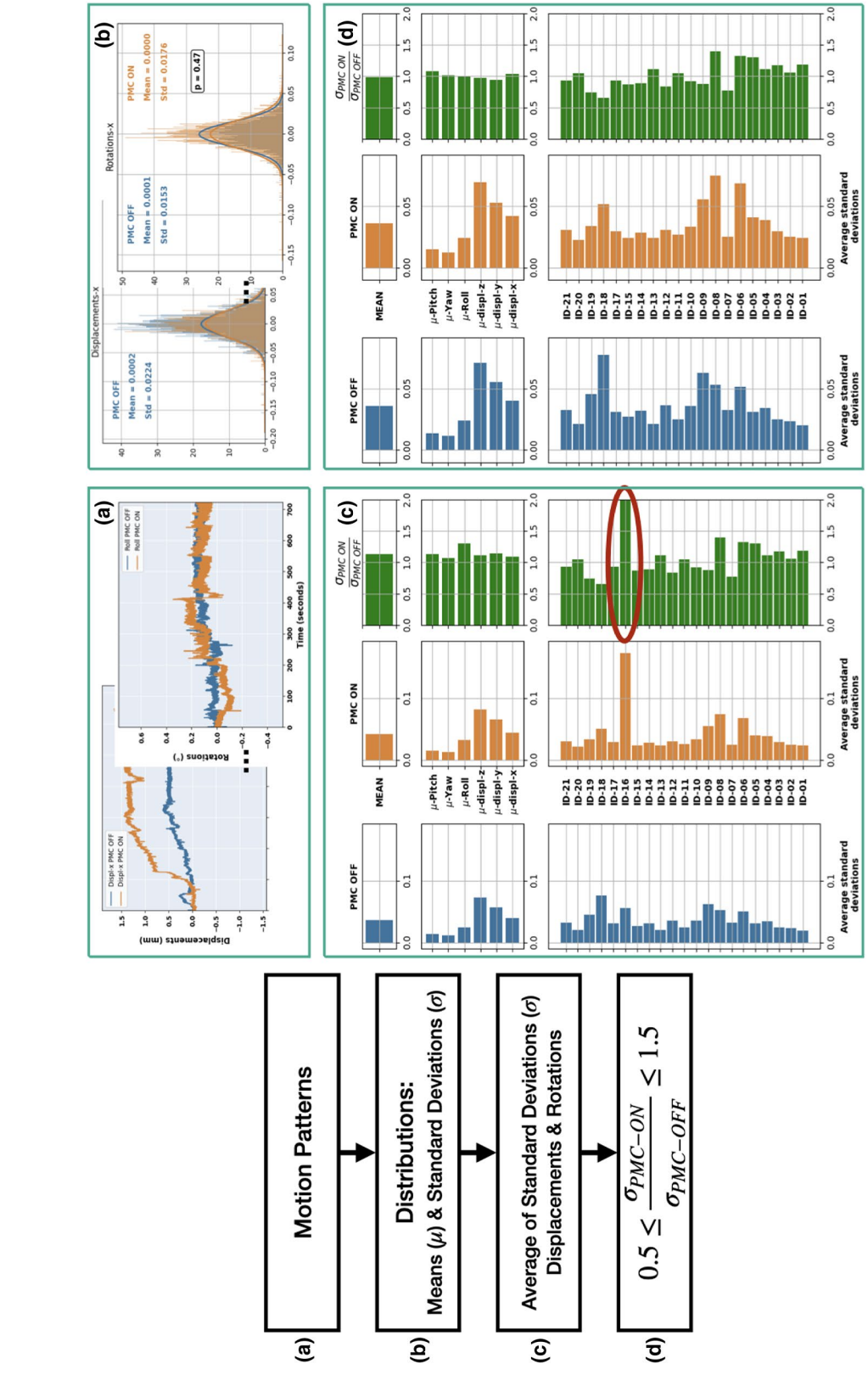

FIGURE 2 Example of motion pattern analysis and exclusion of volumes: motion-tracking data (A), calculation of distributions Equation 1(B); average of SD values of displacements and rotations for each subject/acquisition (C); and filtered volumes, as explained in section 2 (D). Abbreviation: PMC, prospective motion correction

also excluded. Additionally, T_2^*−w (025) of Sub-ID 16 was excluded because of the presence of reflections of the marker, leading to erroneous tracking (Figure 5), which is a limitation of such systems. Reflections occur if the marker is oriented exactly perpendicular to the camera; thus, the marker illumination is reflected into the camera by the marker surface.

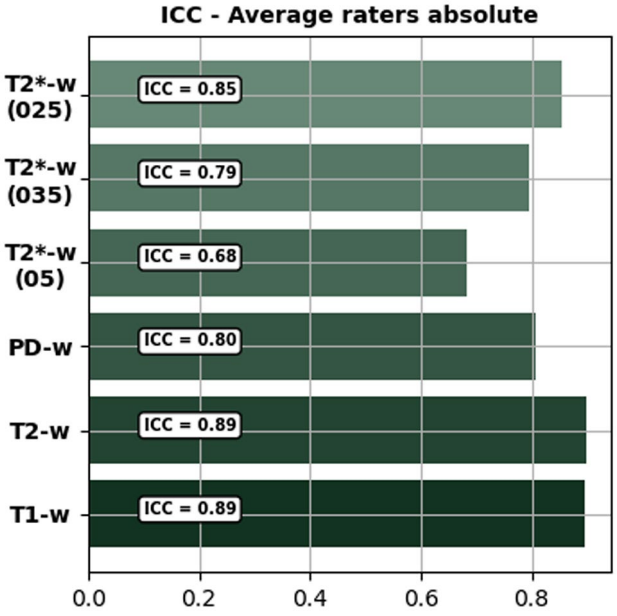

FIGURE 3 Intraclass correlation coefficient (ICC). Average raters' absolute ICC per group. Abbreviations: PD, proton density; T_1-w, T_1-weighted T_2-w, T_2-weighted; T_2^*-w, T_2^*-weighted

3.1 | Subjective image-quality assessment

For each of the 252 image volumes, the four raters assessed the image quality, looking specifically for the presence of motion artifacts. The intraclass correlation coefficient (Figure 3) portrayed that the agreement among the raters was between 0.68 (for T_2^* -w[05]) and 0.89 (for T_1). Considering all contrasts and resolutions together, PMC ON has shown a statistically significant improvement (5.5%) over PMC OFF. The total averaged score and SD were 8.21 ± 0.36 for PMC OFF and 8.77 ± 0.24 for PMC ON, respectively. Details for each group of contrast are reported in Figure 6. The results are shown for each rater and each contrast, including the different resolutions of T_2^*-w images. Moreover, the average scores across all raters are shown. Regarding the T_1, T_2, and PD-w images, the experts awarded a higher score to PMC ON in all cases. For these groups, the PMC ON scans increased in terms of image quality by 9.6%, 9.8% and 9.2%, respectively. The T_2^*-w images did not show statistically significant differences. However, it should be noted that the ratings provided to the images without PMC were already very high (between 8 and 10); hence, the scope for improvement was small.

3.2 | Objective image-quality assessment

For the objective assessment, as described in section 2.3, we used two metrics: the AES and the gradient entropy. Results are shown in Figure 7.

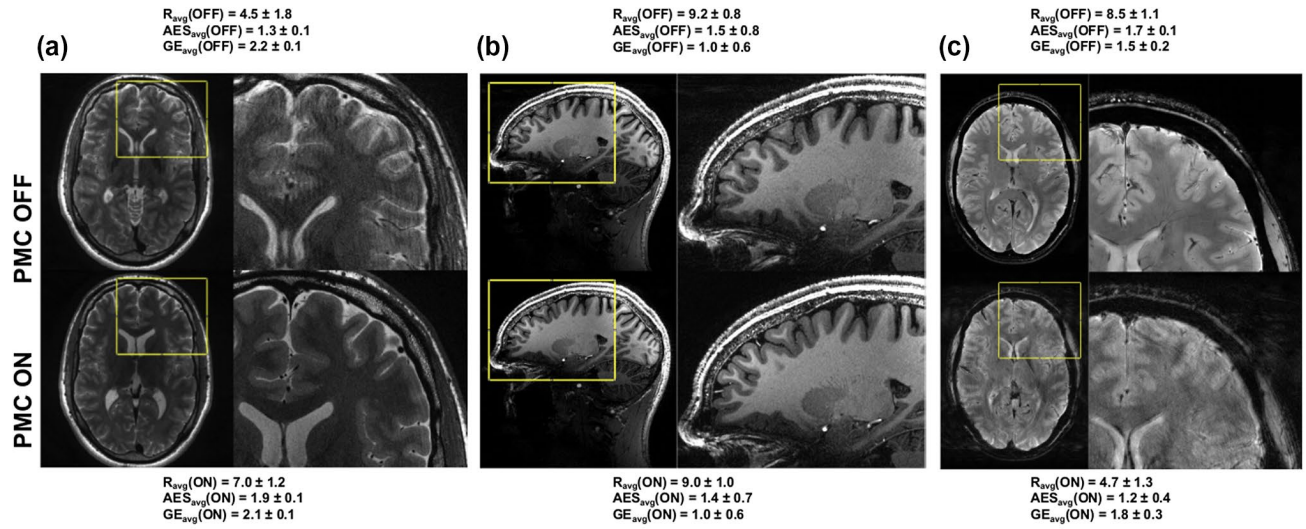

FIGURE 4 Sample images: All three possible scenarios. A, Prospective motion correction OFF performed worse than PMC ON, T_2-weighted images with resolution = 0.28 × 0.28 × 1.0 mm^3. B, Prospective motion correction OFF performed similar to PMC ON, T_1-w images, isotropic resolution over all slices in the volume for average edge strength (AES) and gradient entropy (GE) metrics, respectively (0.45 mm^3). C, Prospective motion correction OFF performed better than PMC ON (reflections in the OMTS system (Figure 5), T_2^*-w images, resolution = 0.25 × 0.25 × 1.5 mm^3. The R_{avg} is the average subjective score, whereas AES_{avg} and GE_{avg} are the average scores over all slices in the volume for AES and gradient entropy metrics, respectively

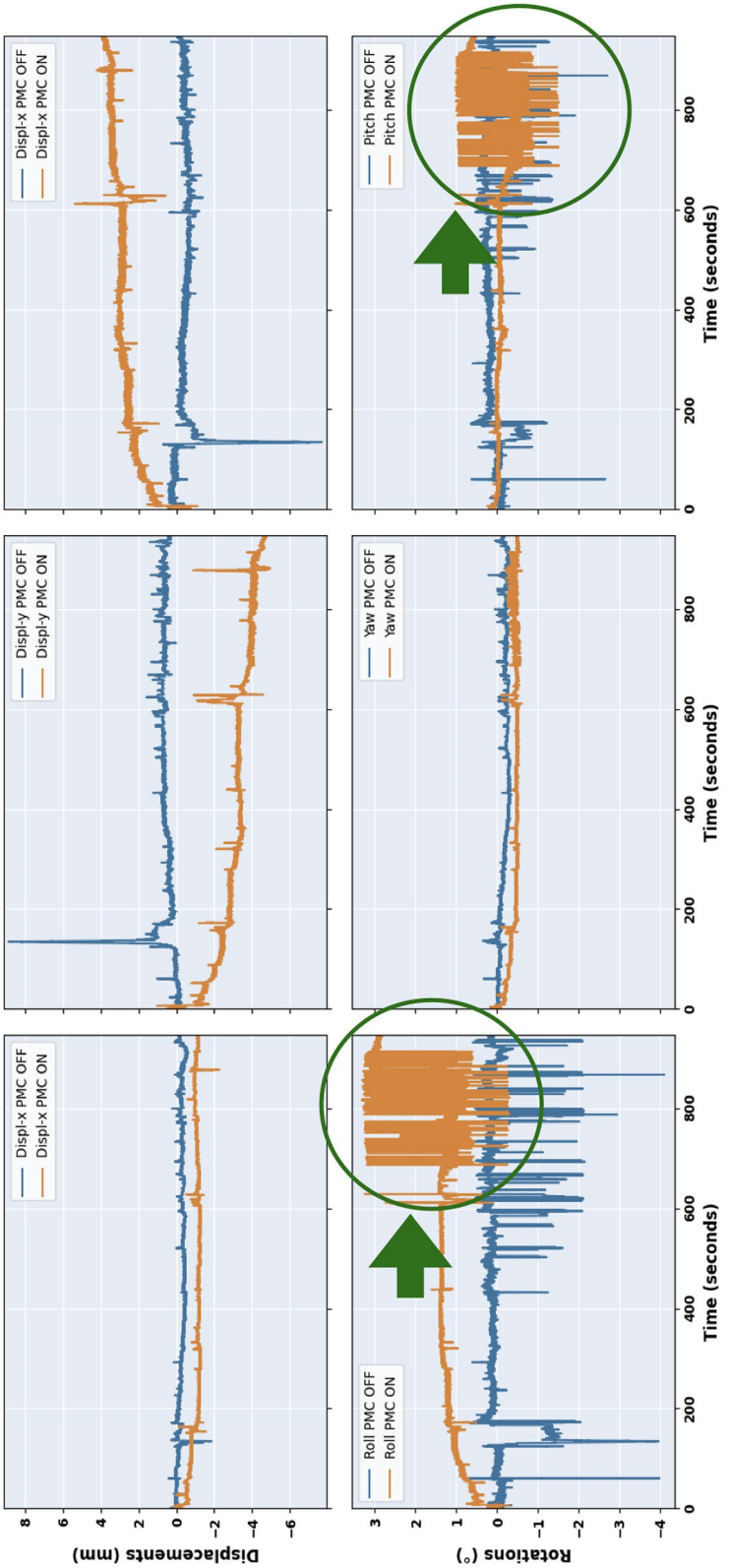

FIGURE 5 Motion patterns in the event of reflections of the MPT marker: false pose data marked with a green circle

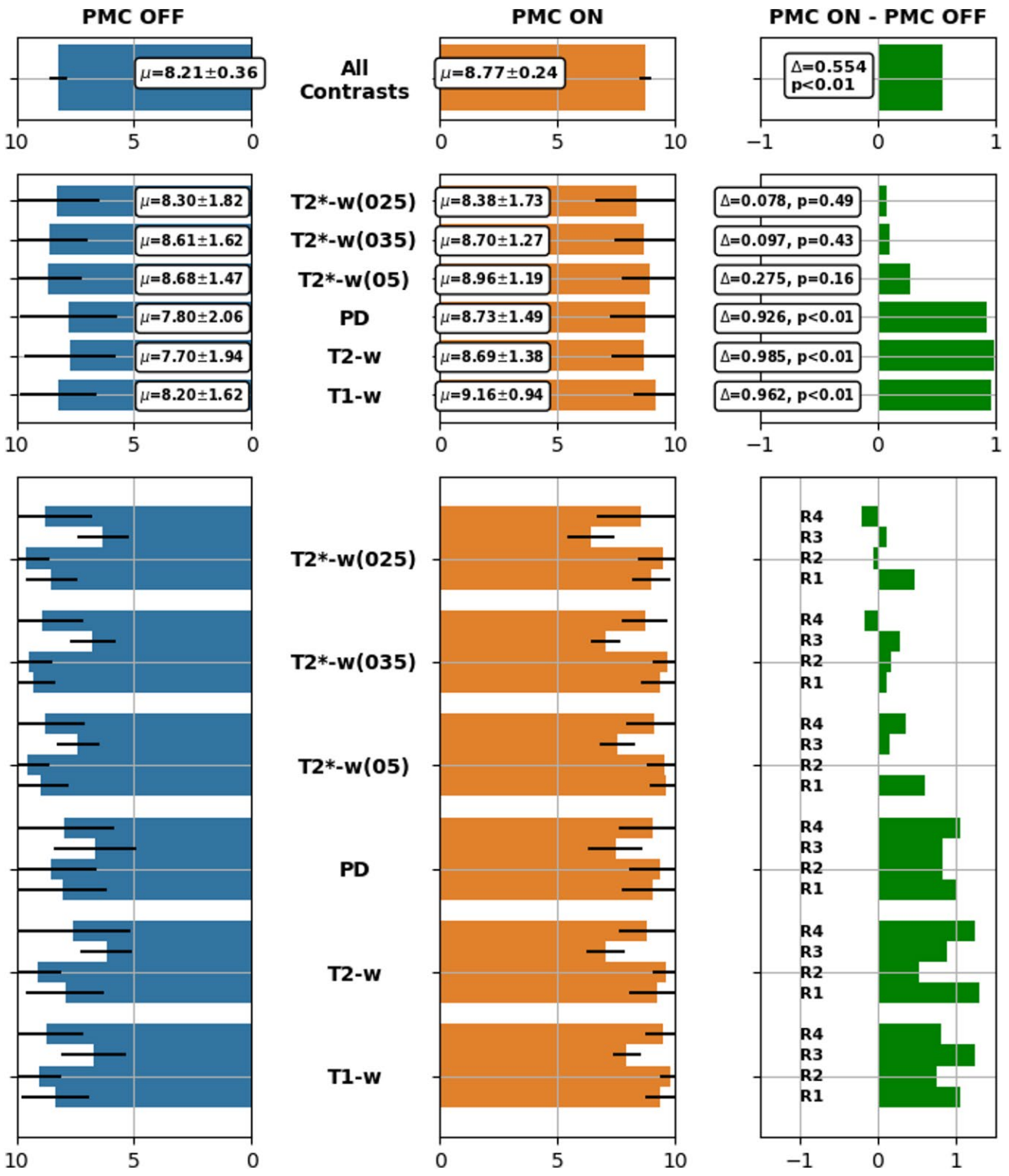

FIGURE 6 Results of the subjective assessment. Bar plots contain average scores calculated for each group and for all groups together. R1, …, R4 refer to reader 1 to reader 4

3.2.1 | Average edge strength

The overall result of AES was statistically significant (6% better) in favor of PMC ON acquisitions. Considering each group separately, only one contrast, T_2^* (025)) has shown a significant statistical improvement with PMC ON of 5.3%. Although not statistically significant, all of the groups have shown improvements with PMC ON, with the only exception being the T_1-w images, in which AES was slightly higher for PMC OFF.

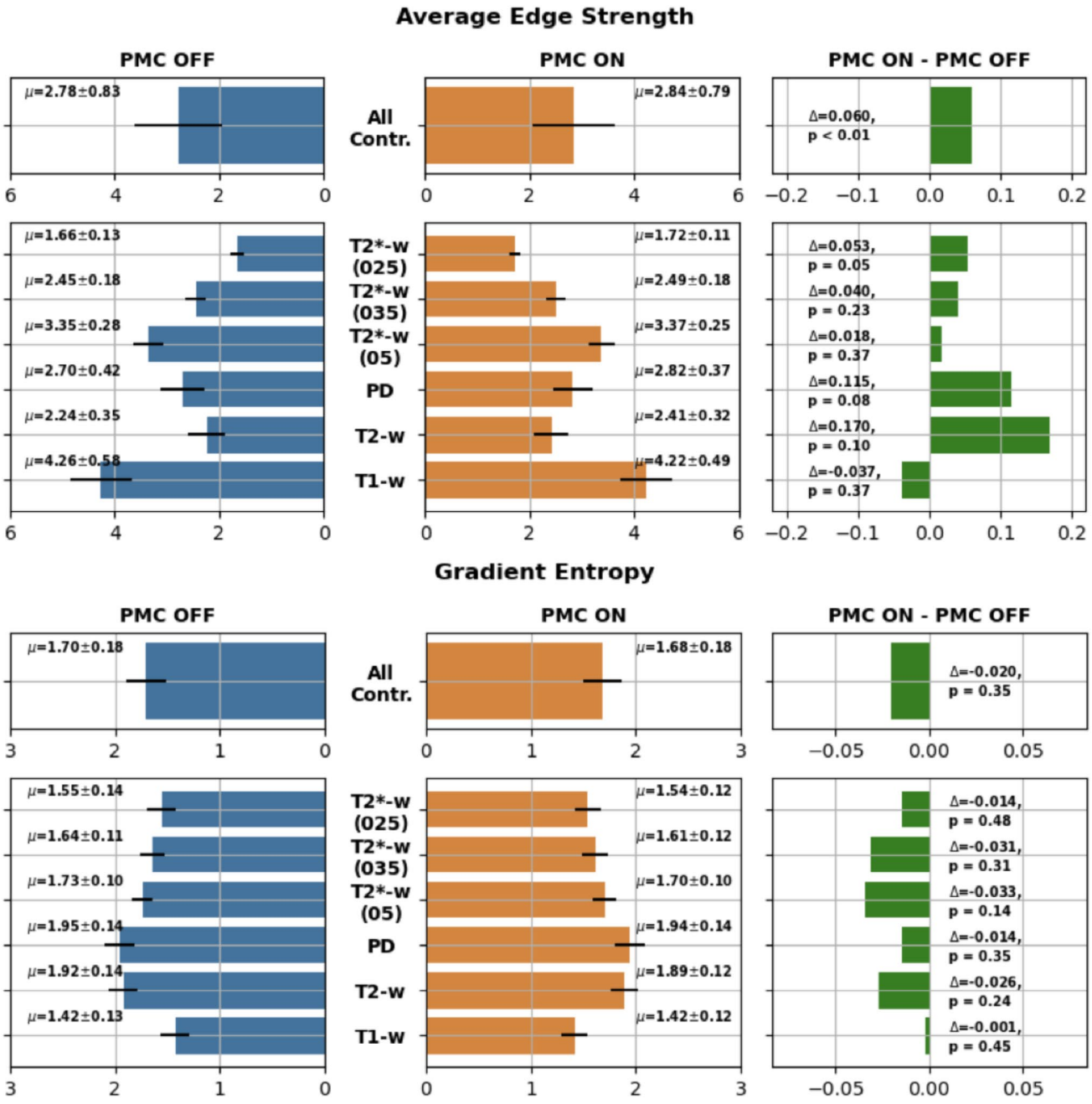

FIGURE 7 Results of the objective assessment. Bar plots contain average scores calculated for each group and for all groups together. Top, AES; bottom, GE

3.2.2 | Gradient entropy

Considering all of the contrasts together and even separately, gradient entropy did not show any statistically significant difference between the two groups—with and without PMC. However, gradient entropy always provided positive results for acquisitions supported by PMC.

4 | DISCUSSION

In this study, an extensive evaluation of PMC has been conducted for structural brain imaging at ultrahigh field in a group of healthy subjects that were instructed to remain as motionless as possible for all scans. Systematic subjective and objective assessments have been performed to compare and quantify the differences in high-resolution in vivo brain images of these healthy compliant subjects acquired with and without PMC.

It was observed in the subjective assessments that the images, whether acquired with or without PMC, received scores mostly between 8 and 10, as reported in Figure 6. Therefore, all images had high to very high image quality, independent of the correction status. However, from the global subjective assessment, it was nonetheless evident that the use of PMC improved the image quality. Looking at the subjective

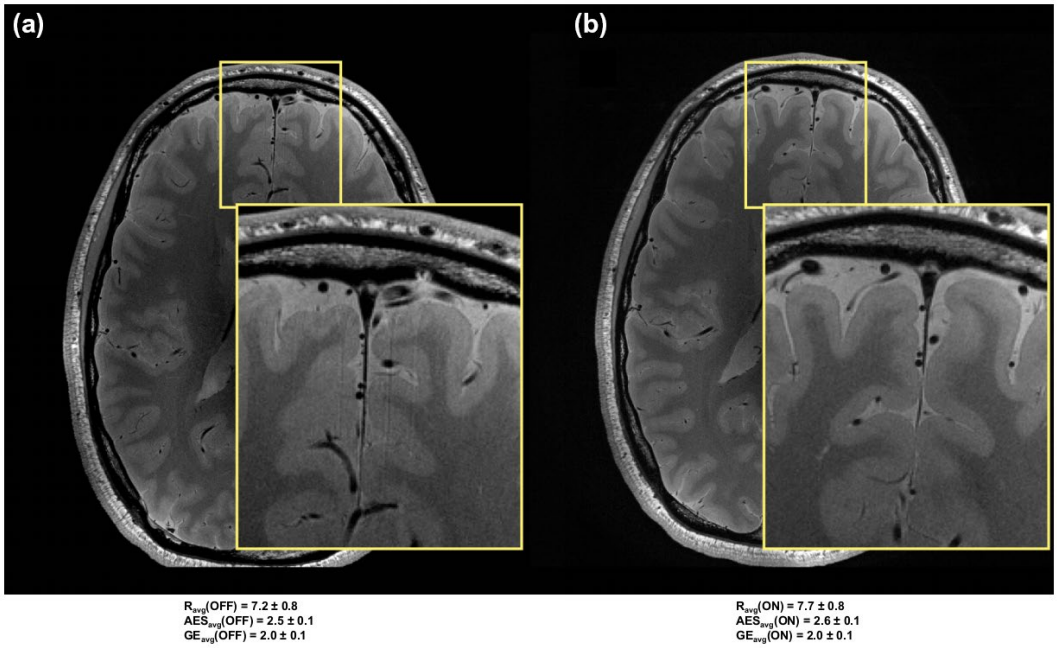

FIGURE 8 Comparison of proton density–weighted (PD-w) images acquired for the same subject. A, Image acquired without the support of PMC. B, Image acquired with PMC. For both images, a zoomed-in area shows the details. The R_{avg}, and the AES_{avg} and GE_{avg} over all slices in these volumes, are reported

evaluation, the positive effect of the use of PMC is statistically significant for three of four contrasts (three of six groups), and for the remaining one contrast (three groups of T_2^*-w images) there was still an improvement, which was not statistically significant. Although all of the experts involved in the evaluation process were experienced in MR image-quality assessment and shared a common training background, the intraclass correlation coefficient varied between 0.68 and 0.89. It is important to reiterate that the task was not only to find whether an image was corrupted or degraded by artifacts, but also to assess the level of degradation. This should be highlighted because it is completely different from what is commonly done in clinical routine, in which scans are assessed within a few seconds to decide whether rescanning is necessary or the image quality is sufficient to perform a clinical diagnosis.

Both objective metrics have shown that the PMC can enhance the image quality for five of six groups (T_2, PD, T_2^* [05], T_2^* [035], and T_2^* [025]). However, for T_1-w images, AES is in favor of PMC OFF and gradient entropy has shown no difference (both not being statistically significant), which is in contradiction to the subjective assessment that showed statistically significant results in favor of PMC ON for this contrast. This generally raises the question of the range of applicability of such metrics for quality assessment of subtle motion artifacts.[25] The results agree with what has been shown in comparable studies. For instance, Mattern et al[14] imaged 4 subjects with a similar sequence (a 3D gradient-echo sequence for susceptibility-weighted imaging, instead of the 2D sequence in our study). In this study, PMC acquisitions with a resolution of $0.33 \times 0.33 \times 1.25$ mm^3 showed a considerable reduction of motion artifacts in most cases and a significant improvement in the reproducibility of quantitative susceptibility values. Stucht et al[1] conducted another comparable study, in which 4 subjects were scanned with similar sequences. Also, in this study, the benefit of PMC was shown in the case of the $0.25 \times 0.25 \times 2.0$ mm^3 gradient-echo (T_2^*-w) images and the 0.44-mm^3 isotropic T_1-w images. However, these studies cannot be considered fully comparable in terms of the number of subjects scanned, and the number and type of sequences acquired per subject.

Although we tested all of the sequences on a phantom to verify the impact of vibrations and observed that the gradients did not affect the motion patterns or image quality, we cannot prove that the same is valid for in vivo imaging. Experimental differences, such as the loading conditions of the patient table, may lead to differences in the mechanical properties and coupling of the setup. Furthermore, different mounting conditions may affect the performance of the optical tracking system. In general, we did not observe any anomalies in the tracking information to indicate possible PMC malfunctions or erroneous tracking, except in one acquisition (discussed in section 3 and shown in Figure 5). As described in section 2, the OMTS was mounted using Velcro straps (Figure 1). We did not investigate whether the Velcro can assure that the mechanical properties and orientation of the camera are stable over the course of a scan and between scans. The same concern exists with respect to the gradual degradation of the

Velcro with repeated use. This could lead to different mounting conditions and consequently affect the performance of the optical tracking system. Furthermore, differences in contrast and SNR could potentially affect the results obtained by the objective evaluation.[26,27] It is noteworthy that in certain cases (shown in Figure 8), reduction in artifacts became obvious in the PMC-ON image only following close inspection.

Based on our results, PMC using an OMTS can improve the image quality of already very good images of healthy compliant subjects without intentional motion during the scan.

5 | CONCLUSIONS

This paper presents a large-scale study on PMC to systematically assess high-resolution MRIs at 7 T in cooperative subjects. Most of the acquired images presented a high or very high image quality. Subjective assessment has shown improvement with PMC ON for every scenario, but only three of them were also statistically significant. Objective metrics have shown that the images acquired with PMC were better in terms of image quality for five of six groups; for the final group, the metrics did not agree on a clear winner and were not consistent with the subjective metric. Only the images with similar motion patterns for both PMC ON and OFF were considered in the analysis here. Hence, the improvements observed can be attributed to PMC. Based on our results, we conclude that PMC provides better image quality for high-resolution images in the absence of intentional motion, and it should be taken into consideration even when acquiring high-resolution scans at 7 T of healthy compliant subjects.

ACKNOWLEDGMENT

The authors thank the staff of the Department of Oral and Maxillofacial Surgery, University Hospital Magdeburg A.ö.R., Christian Zahl, Indra Griesau, and Christine Rohloff for creating individually custom-made removable dental braces. Open Access funding enabled and organized by Projekt DEAL.

ORCID

Alessandro Sciarra https://orcid.org/0000-0002-1247-2772
Hendrik Mattern https://orcid.org/0000-0001-5740-4522
Soumick Chatterjee https://orcid.org/0000-0001-7594-1188

REFERENCES

1. Stucht D, Danishad KA, Schulze P, Godenschweger F, Zaitsev M, Speck O. Highest resolution in vivo human brain MRI using prospective motion correction. *PloS ONE*. 2015;10:e0133921.
2. Herbst M, Maclaren J, Lovell-Smith C, et al. Reproduction of motion artifacts for performance analysis of prospective motion correction in MRI. *Magn Reson Med*. 2014;71:182-190.
3. Lee CC, Jack CR, Grimm RC, et al. Real-time adaptive motion correction in functional MRI. *Magn Reson Med*. 1996;36:436-444.
4. Maclaren J, Herbst M, Speck O, Zaitsev M. Prospective motion correction in brain imaging: a review. *Magn Reson Med*. 2013;69:621-636.
5. Pannetier NA, Stavrinos T, Ng P, et al. Quantitative framework for prospective motion correction evaluation. *Magn Reson Med*. 2016;75:810-816.
6. Haacke EM, Patrick JL. Reducing motion artifacts in two-dimensional Fourier transform imaging. *Magn Reson Imaging*. 1986;4:359-376.
7. Godenschweger F, Kägebein U, Stucht D, et al. Motion correction in MRI of the brain. *Phys Med Biol*. 2016;61:R32-R56.
8. Zaitsev M, Dold C, Sakas G, Hennig J, Speck O. Magnetic resonance imaging of freely moving objects: prospective real-time motion correction using an external optical motion tracking system. *Neuroimage*. 2006;31:1038-1050.
9. Maclaren J, Speck O, Stucht D, Schulze P, Hennig J, Zaitsev M. Navigator accuracy requirements for prospective motion correction. *Magn Reson Med*. 2010;63:162-170.
10. Zaitsev M, Maclaren J, Herbst M. Motion artefacts in MRI: a complex problem with many partial solutions. *J Magn Reson Imaging: JMRI*. 2015;42:887-901.
11. Singh A, Zahneisen B, Keating B, et al. Optical tracking with two markers for robust prospective motion correction for brain imaging. *Magma (New York, NY)*. 2015;28:523-534.
12. Eschelbach M, Aghaeifar A, Bause J, et al. Comparison of prospective head motion correction with NMR field probes and an optical tracking system. *Magn Reson Med*. 2019;81:719-729.
13. Gretsch F, Mattern H, Gallichan D, Speck O. Fat navigators and Moiré phase tracking comparison for motion estimation and retrospective correction. *Magn Reson Med*. 2020;83:83-93.
14. Mattern H, Sciarra A, Lüsebrink F, Acosta-Cabronero J, Speck O. Prospective motion correction improves high-resolution quantitative susceptibility mapping at 7T. *Magn Reson Med*. 2019;81:1605-1619.
15. Lüsebrink F, Sciarra A, Mattern H, Yakupov R, Speck O. T1-weighted in vivo human whole brain MRI dataset with an ultrahigh isotropic resolution of 250 um. *Scientific Data*. 2017;4:170032 EP.
16. Mattern H, Sciarra A, Godenschweger F, et al. Prospective motion correction enables highest resolution time-of-flight angiography at 7T. *Magn Reson Med*. 2018;80:248-258.
17. Maclaren J, Armstrong BSR, Barrows RT, et al. Measurement and correction of microscopic head motion during magnetic resonance imaging of the brain. *PLoS One*. 2012;7:e48088.
18. Mann HB, Whitney DR. On a test of whether one of two random variables is stochastically larger than the other. *Ann Math Stat*. 1947;50-60.
19. Bartko JJ. The intraclass correlation coefficient as a measure of reliability. *Psychol Rep*. 1966;19:3-11.
20. Shrout PE, Fleiss JL. Intraclass correlations: uses in assessing rater reliability. *Psychol Bull*. 1979;86:420.
21. Vallat R. Pingouin: statistics in Python. *J Open Source Softw*. 2018;3:1026.
22. Esteban O, Birman D, Schaer M, Koyejo OO, Poldrack RA, Gorgolewski KJ. MRIQC: advancing the automatic prediction of image quality in MRI from unseen sites. *PLoS One*. 2017;12:1-21.
23. McGee KP, Manduca A, Felmlee JP, Riederer SJ, Ehman RL. Image metric-based correction (autocorrection) of motion effects: analysis of image metrics. *J Magn Reson Imaging*. 2000;11:174-181.

24. Woodard JP, Carley-Spencer MP. No-reference image quality metrics for structural MRI. *Neuroinformatics*. 2006;4:243-262.
25. Bazin P-L, Nijsse HE, van der Zwaag W, et al. Sharpness in motion corrected quantitative imaging at 7T. *Neuroimage*. 2020;222:117227.
26. Chow LS, Paramesran R. Review of medical image quality assessment. *Biomed Signal Process Control*. 2016;27:145-154.
27. Krbcova Z, Kukal J. Relationship between entropy and SNR changes in image enhancement. *EURASIP J Image Video Process*. 2017;2017:83.

How to cite this article: Sciarra A, Mattern H, Yakupov R, et al. Quantitative evaluation of prospective motion correction in healthy subjects at 7T MRI. *Magn Reson Med*. 2022;87:646–657. https://doi.org/10.1002/mrm.28998